Int J Earth Sciences (Geol Rundsch) (2001) 90 : 703–713
DOI 10.1007/s005310000184

ORIGINAL PAPER

Britta Trautwein · István Dunkl · Wolfgang Frisch

Accretionary history of the Rhenodanubian flysch zone in the Eastern Alps – evidence from apatite fission-track geochronology

Received: 17 May 2000 / Accepted: 15 November 2000 / Published online: 15 March 2001

Abstract The thermotectonic evolution of the East Alpine Rhenodanubian flysch zone (RDFZ) and the collisional history along the orogenic front is reconstructed using apatite fission-track (FT) thermochronology. The apatite FT data provides evidence for a burial depth of at least 6 km for the samples, which were totally reset. Burial was not deeper than 11 km, since the zircon fission-track system was not reset. The RDFZ represents an accretionary wedge with a complex burial and cooling history due to successive and differential accretion and exhumation. The sedimentary sequences were deposited along a convergent margin, where accretion started before Maastrichtian and lasted until Miocene. Accretion propagated from a central area (Salzburg–Ybbsitz) both to the west and to the east. In the west, accretion lasted from Middle Eocene to Early Oligocene, reflecting underplating of the RDFZ by the European continental margin sediments. In the east, where three nappes (Greifenstein, Kahlenberg and Laab nappes) can be distinguished, the exhumation started between Late Oligocene and Early Miocene. The Kahlenberg and Laab nappes show total resetting of the apatite FT ages, while in the Greifenstein nappe there is only partial resetting. According to a new paleogeographic reconstruction, the Kahlenberg and Laab nappes were placed on top of the Greifenstein nappe by an out-of-sequence thrust.

Keywords Rhenodanubian flysch zone · Eastern Alps · Apatite fission-track thermochronology · Nappe accretion · Paleogeography

B. Trautwein (✉) · I. Dunkl · W. Frisch
Geologisches und Paläontologisches Institut, Sigwartstr. 10, 72076 Tübingen, Germany
E-mail: britta.trautwein@uni-tuebingen.de
Phone: +49-7071-2974702
Fax: +49-7071-5059

Introduction

The Rhenodanubian flysch zone (RDFZ) is very important for any geodynamic reconstruction of the pre- and syn-collisional history of the Eastern Alps. Its sedimentary characteristics and its clastic material provide information about its geotectonic position. The aim of this apatite fission-track (FT) study is to reconstruct the thermal evolution of the Rhenodanubian flysch zone during and after collision of the Alpine orogen, and to evaluate the consequences for the paleogeographic reconstruction.

Geological setting

The Rhenodanubian flysch zone forms a ~500-km-long and narrow unit along the northern front of the Eastern Alps (Fig. 1). It contains mostly turbiditic sequences of Early Cretaceous to Middle Eocene age (Fig. 2), which were deposited in a basin with partly oceanic and partly thinned continental crust (Egger 1990, 1992; Schnabel 1992). Schnabel (1992) suggested that the Ybbsitz klippen zone (YKZ), which is correlated with the St. Veit klippen zone and the Kahlenberg nappe (Schnabel 1979, 1992; Exner and Kirchner 1982), contains the oceanic basement of the Rhenodanubian flysch trough. The Ybbsitz klippen zone consists of a Jurassic deep-sea facies with radiolarites, mafic/ultramafic rocks, pillow basalts, serpentinites and ophicalcites, and a flysch cover of Cretaceous age (Schnabel 1979; Ruttner and Schnabel 1988; Decker 1990).

The Rhenodanubian flysch zone belongs to the Penninic paleogeographic realm of the Alps, but its exact position is still a matter of discussion (e.g. Hesse 1973; Frisch 1979; Winkler et al. 1985; Egger 1992; Faupl and Wagreich 1992; Oberhauser 1995). It forms a north-vergent fold-and-thrust belt and is sandwiched

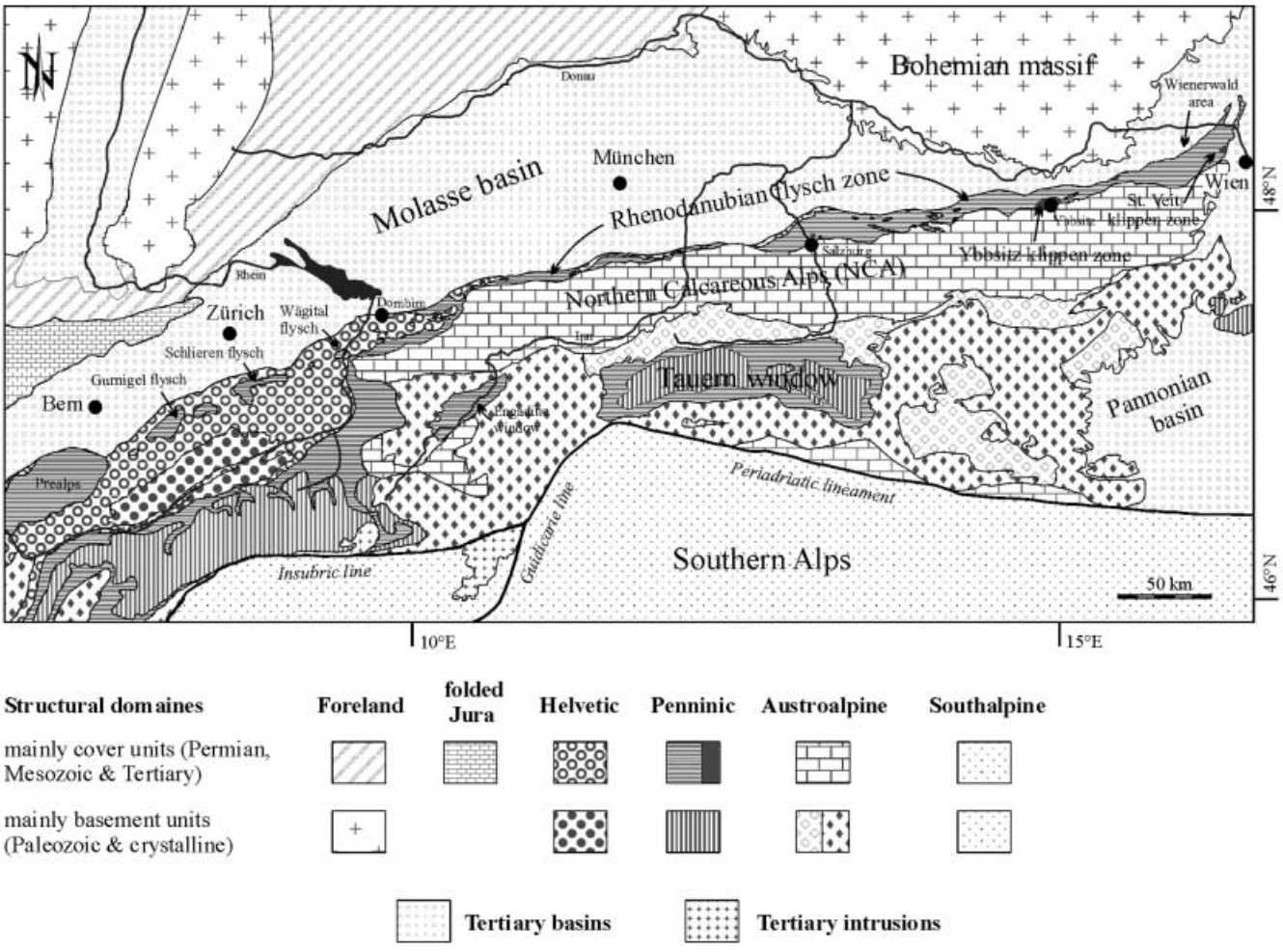

Fig. 1 Geological map of the Central and Eastern Alps showing the position of Rhenodanubian flysch and Ybbsitz klippen zone

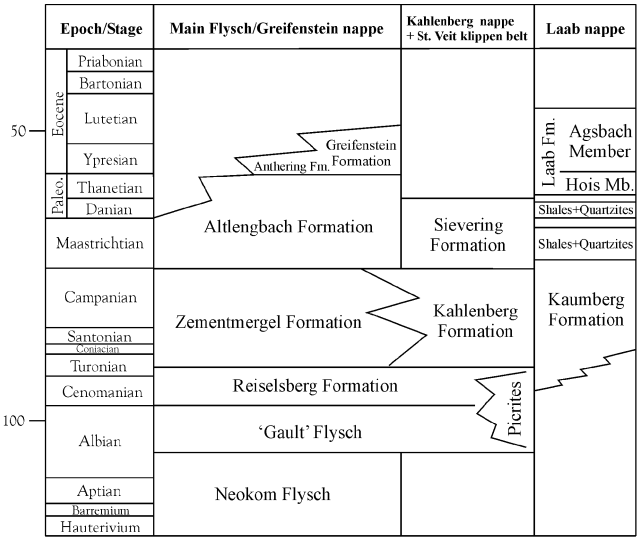

Fig. 2 Simplified stratigraphic scheme of the Rhenodanubian flysch zone after Prey (1980), Plöchinger and Prey (1993), Egger (1995) and Faupl (1996)

between the overlying nappe stack of the Northern Calcareous Alps and the underlying folded and parautochthonous Molasse zone. The RDFZ is the product of thin-skinned tectonics, which also incorporated the Ultrahelvetic units of the southern European margin.

The Rhenodanubian flysch zone is strongly sliced and tectonically disrupted. The Main Flysch nappe stretches over the whole length of the zone from the Rhine River to the Danube River. In the central and western part, it has been subdivided into several subnappes (Hesse 1972; von Rad 1972; Egger 1989; Mattern 1998). In the Wienerwald area, the RDFZ is subdivided into three nappes. The Greifenstein nappe, which is the equivalent of the Main Flysch nappe (Schnabel 1992), is overlain by the Laab nappe in the south and by the Kahlenberg nappe in the southeast (Fig. 3). The latter occupies the highest structural position (Prey 1983). These tectono-stratigraphic units are assumed to have been deposited in separate basins (e.g. Faupl and Wagreich 1992; Schnabel 1992; Faupl 1996).

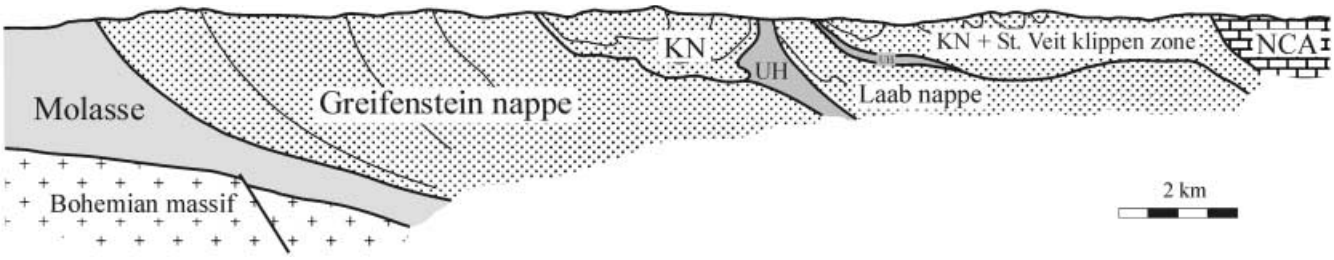

Fig. 3 Schematic arrangement of the Wienerwald nappe pile after Prey (1980). *NCA* Northern Calcareous Alps, *UH* Ultrahelvetic units, *KN* Kahlenberg nappe

Methods

The apatite FT dating method is widely used to date the low-temperature cooling history of rocks (e.g. Wagner and Van den haute 1992). In the case of sedimentary sequences that were buried and heated above ~100 °C, their thermal history can be constrained. Fission-track length measurements help to interpret the apparent apatite ages, and to elucidate the basin evolution (Green 1986). Since the apatites of the Rhenodanubian flysch units are thermally reset, a possible thermal evolution of the RDFZ can be reconstructed.

FT ages were determined using the external-detector method (Gleadow 1981). A pooled age is calculated in the case of a homogeneous population, i.e. where the sample passes the χ^2 test (Galbraith 1981). If it fails the χ^2 test, a mean age is calculated (Green 1981).

The study of FT length distributions in apatite has the potential for providing constraints on the time–temperature history of a rock under low-temperature conditions. Progressive annealing during increasing temperature reduces the length of the fission tracks until tracks are totally erased. In thermally overprinted sedimentary basins, the ratio of inherited to newly formed tracks depends on the amount of annealing.

The apatite samples were counted with ×1000 magnification using immersion oil. For the track-length measurements Tints (track-in-track) and Tincles (track-in-cleavage) were considered (Bhandari et al. 1971).

In order to judge whether the variation in the fission-track ages is dependent on differential annealing behaviour due to differences in chemistry, the fluorine and chlorine contents were measured by electron microprobe. The concentrations of F, Cl and OH influence the annealing temperature. Fluorine apatite is much less resistant to annealing than chlorine apatite (Green et al. 1986, 1989; Green 1988). The analyses were performed on a Cameca SX51 spectrometer at an acceleration voltage of 15 kV, a probe current of 20 nA and a defocused spot of 20 μm.

Laboratory, experimental and calculation procedures of the fission-track and microprobe measurements, as well as the apatite fission-track distributions are described in more detail in Trautwein (2000).

Results

Thirty-six samples were collected in Cenomanian to Eocene units of the Rhenodanubian flysch zone including a picritic dyke, which intruded into mid-Cretaceous strata of the RDFZ. Two samples were taken from units of the Ybbsitz klippen zone (Table 1).

The apatite populations of the sedimentary units contain both rounded and subhedral grains. Some crystals show overgrowth rims. Most apatites are clear and colourless, but reddish-brown and greyish-black varieties are also common. The apatite grains of the picritic dyke (sample no. 36) are of subhedral shape. They show brownish circular tubes, which are characteristic of volcanic apatites.

Apatite fission-track ages

Apatite FT age determination was carried out on 36 samples from the Rhenodanubian flysch zone and two samples from the Ybbsitz klippen zone (Table 1, Fig. 4a). The determined ages are so-called apparent ages. Depending on the time–temperature evolution, they reflect cooling of the sediments, mixed ages with an inherited history, or purely inherited ages without overprint (Fig. 4a).

The apatite FT ages of the Main Flysch/Greifenstein nappe vary along strike from west to east. Miocene and Oligocene ages are found for the westernmost samples and samples along the southern margin of the Main Flysch nappe (Fig. 4a, b). Apatite ages from the Rhenodanubian flysch zone along the Rhine valley (~18 and 19 Ma; Rahn, personal communication) are in good agreement with the data presented here from the westernmost part of the RDFZ. In the central part and in the vicinity of the Ybbsitz klippen zone (YKZ), the FT ages become older (Late Cretaceous to Eocene). Apatite FT dating in the central RDFZ was earlier performed by Hejl and Grundmann (1989), using the population method. In their study, they determined an apatite FT age of 106 Ma for the same locality as sample no. 14 in this study. The sig-

Table 1 Apatite fission-track ages and track-length parameters. The ages were calculated using a ζ-factor of 380.4±6.5. The ζ-value was calculated from 13 different age standards of Fish Canyon Tuff and Durango apatite. *Ce* Cenomanian, *Tu* Turonian, *Co* Coniacian, *Sa* Santonian, *Ca* Campanian, *Ma* Maastrichtian, *Pa* Paleocene, *Eo* Eocene, ρ track density, *N* number of counted tracks

							Spontaneous tracks		Induced tracks		Dosimeter glass (CN5)						Measurements of confined fission tracks		
Sample no.	Formation	Sedimentation age	Locality		Alt.	No. of crystals	ρ_s	N_s	ρ_i	N_i>	ρ_d	N_d	P(χ^2)	ρ_s/ρ_i	Age±1σ	U (ppm)	No. of length	Mean track length	SD
			N	E	(m)		(10^5/cm^2)		(10^5/cm^2)		(10^5/cm^2)		(%)		(Ma)	[V.C. (%)]		(µm)	(µm)
Rhenodanubian flysch zone																			
Main Flysch/Greifenstein nappe																			
1	Altlengbach	Ma	47°37′30″	10°50′32″	1260	48	20.138	1069	17.866	959	5.24	10395	0.01	1.247	123.1±3.5	41.49 (±63)	-	-	-
2	Altlengbach	Ma	47°17′39″	10°02′36″	920	39	3.833	211	16.146	957	4.59	8938	28.14	-	19.2±1.5	42.81 (±78)	-	-	-
3	Reiselsberg	Ce–Tu	47°42′52″	11°46′48″	845	56	2.411	227	7.338	741	5.24	10395	89.39	-	30.5±2.4	17.04 (±133)	30	14.0	1.3
4	Reiselsberg	Ce–Tu	47°37′06″′	10°57′42″	938	55	3.133	319	9.73	1082	5.24	10395	20.49	-	29.3±2.0	22.6 (±173)	34	13.8	1.2
5	Reiselsberg	Ce–Tu	47°28′25″	10°10′19″	1120	58	1.358	179	7.88	1084	5.24	10395	68.48	-	16.4±1.4	18.3 (±123)	43	13.8	1.9
6	Altlengbach	Ma	47°53′59″	13°23′15″	788	46	8.698	1213	11.909	1975	5.21	10345	0	0.596	58.8±1.7	27.82 (±73)	63	11.9	2.0
7	Altlengbach	Ma	47°55′15″	13°45′55″	670	49	6.328	1011	9.927	1680	4.55	9175	0.02	0.614	52.9±1.5	26.55 (±85)	101	12.6	2.2
8	Altlengbach	Ma	47°53′32″	13°37′23″	580	55	15.053	2091	16.264	2483	4.842	9543	0	0.88	80.6±2.3	40.88 (±71)	-	-	-
9	Altlengbach	Ma	47°55′15″	13°45′55″	670	44	7.851	518	14.578	996	4.858	9543	0.23	0.622	57.2±1.8	36.52 (±74)	-	-	-
10	Altlengbach	Ma	47°55′15″	13°45′55″	670	55	9.118	904	15.727	1673	4.863	9543	0	0.581	53.5±1.5	39.36 (±133)	74	12.1	2.5
11	Altlengbach	Ma	47°47′12″	12°55′29″	740	60	23.504	2055	17.753	1738	5.24	10395	0	1.273	125.7±3.3	41.23 (±79)	-	-	-
12	Reiselsberg	Ce–Tu	47°49′48″	13°26′59″	760	45	4.416	790	6.04	1033	4.55	9175	0	0.685	59.0±1.8	16.16 (±96)	101	12.4	1.7
13	Reiselsberg	Ce–Tu	47°47′39″	12°37′00″	820	51	1.442	409	5.532	1602	5.21	10345	70.69	-	25.2±1.5	12.92 (±104)	30	13.6	1.3
14	Reiselsberg	Ce–Tu	47°48′35″	13°25′05″	500	48	4.959	1513	8.024	2377	4.836	9543	0	0.625	57.2±1.8	20.19 (±98)	50	12.6	2.4
15	Reiselsberg	Ce–Tu	47°51′53″	13°37′13″	750	45	2.795	617	8.425	1905	4.873	9543	2.57	0.31	28.7±0.9	21.04 (±84)	31	14.0	1.2
16	Reiselsberg	Ce–Tu	47°47′02″	12°40′28″	1038	46	2.578	457	5.978	1037	4.55	9175	36.84	-	38.0±2.3	15.99 (±114)	37	13.3	2.4
17	Greifenstein	Pa–Eo	48°04′16″	15°28′58″	360	60	4.22	822	14.828	2970	4.59	8938	0.98	0.283	24.6±0.6	39.32 (±73)	50	13.7	1.9
18	Altlengbach	Ma	47°59′06″	14°57′58″	760	60	8.01	623	15.134	1375	4.59	8938	0	0.528	46.0±1.2	40.13 (±68)	54	12.3	2.7
19	Altlengbach	?Ca–Ma	47°59′49″	14°55′58″	490	60	4.098	546	10.619	1414	4.59	8938	0.01	0.389	33.9±0.9	28.15 (±67)	56	12.7	2.2
20	Reiselsberg	Ce–Tu	47°58′22″	14°51′01″	455	31	2.125	151	7.304	471	5.24	10395	35.07	-	31.9±3.0	16.96 (±101)	11	13.1	2.1
21	Reiselsberg	Ce–Tu	47°58′51″	14°52′43″	500	56	7.756	745	9.029	962	5.24	10395	0	0.874	86.5±2.3	20.97 (±79)	100	12.6	1.7
22	Greifenstein	Eo	48°20′57″	15°15′34″	200	35	18.353	594	12.073	402	5.24	10395	0.17	1.382	136.3±4.8	28.04 (±90)	-	-	-
23	Altlengbach	Ma	48°19′13″	16°12′44″	240	58	16.026	564	20.217	758	5.24	10395	0	0.777	76.9±2.0	46.95 (±86)	48	11.1	1.9
24	Altlengbach	Ma	48°10′32″	16°03′47″	350	56	13.725	694	13.413	829	5.24	10395	0	0.939	92.9±2.5	31.15 (±102)	66	11.8	1.9
Laab nappe																			
25	Laab	Pa	48°01′48″	15°58′37″	420	75	3.779	520	17.061	2258	5.24	10395	7.45	-	22.9±1.2	39.62 (±96)	50	13.8	2.1
26	Laab	Pa	48°03′21″	15°56′26″	511	58	3.506	417	18.061	2184	5.24	10395	14.93	-	19.0±1.1	41.95 (±83)	63	14.3	1.9
27	Kaumberg	Co–Sa	48°03′11″	15°56′41″	490	25	5.74	156	25.059	673	4.59	8938	16.18	-	20.2±1.8	66.44 (±71)	-	-	-
Kahlenberg nappe																			
28	Sievering	Ma	48°15′30″	16°17′55″	403	60	1.9	258	9.143	1238	5.24	10395	7.23	-	20.7±1.5	21.23 (±117)	36	13.8	1.9
29	Sievering	Ma	48°13′50″	16°14′32″	315	20	3.585	131	13.941	549	5.24	10395	77.15	-	23.7±2.4	32.38 (±96)	-	-	-
30	Sievering	Ma	48°12′17″	16°12′27″	275	60	2.576	483	13.401	2445	5.24	10395	61.65	-	19.7±1.1	31.12 (±76)	-	-	-
31	Kahlenberg	Ca	48°11′35″	16°08′45″	275	35	2.993	363	11.387	1423	5.24	10395	0.58	0.255	25.4±0.9	26.45 (±68)	-	-	-
32	Kahlenberg	Sa–Ca	48°16′55″	16°20′24″	412	53	4.118	395	15.74	1575	5.24	10395	14.25	-	24.9±1.5	36.56 (±92)	39	13.3	2.1
33	Kahlenberg	Sa–Ca	48°12′52″	16°12′29″	260	35	2.3	233	9.772	1079	5.24	10395	2.34	0.231	23.0±0.8	22.69 (±81)	-	-	-
34	Kahlenberg	Sa	48°16′38″	16°21′10″	300	52	3.789	396	17.96	1988	4.884	9543	0.27	0.199	18.5±0.5	44.75 (±88)	10	14.5	1.7
35	Reiselsberg	Ce–Tu	48°12′37″	16°15′31″	300	55	1.35	104	6.631	568	5.24	10395	74.63	-	18.2±2.0	15.4 (±94)	21	14.1	2.4
36	Picrite, mid-Cretaceous		48°12′38″	16°17′24″	230	46	1.878	120	5.892	391	4.59	8938	96.02	-	26.7±2.8	15.62 (±47)	58	14.9	1.6
Ybbsitz klippen zone																			
37	Steinkeller	Sa–Ca	47°58′30″	14°55′50″	560	54	4.769	494	19.073	2101	5.24	10395	11.65	-	23.4±1.3	44.3 (±77)	64	13.3	1.8
38	Hubberg	Ce–Co	47°57′52″	14°53′06″	560	58	8.829	726	19.759	1803	5.24	10395	0.18	0.416	41.3±1.1	45.89 (±77)	94	12.4	2.5

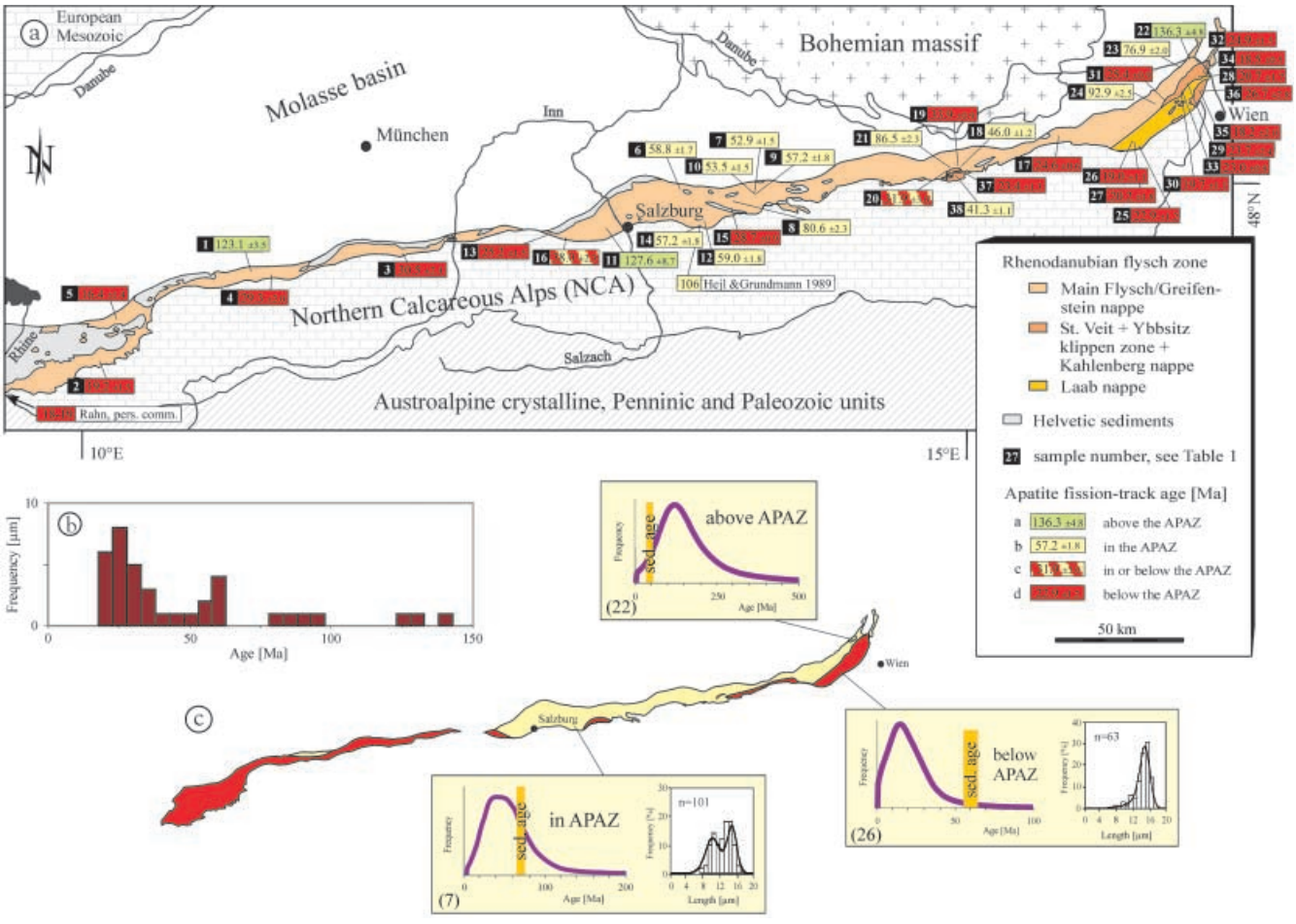

Fig. 4 **a** Apatite fission-track ages in the Rhenodanubian flysch and Ybbsitz klippen zone, grouped on the basis of their burial depth; *APAZ* apatite partial annealing zone; **b** age distribution in the Rhenodanubian flysch and Ybbsitz klippen zone; **c** population density curves (Hurford et al. 1984) of representative samples from above, within and below the APAZ

nificant difference in age might be due to the different methods used. At the eastern end of the RDFZ in the Wienerwald area, the apatite fission-track ages vary between 77 and 136 Ma in the Altlengbach and Greifenstein formation of the Greifenstein nappe.

The Cenomanian to Maastrichtian formations of the Kahlenberg nappe display apatite FT ages between 18 and 25 Ma. The apatite fission-track age of the picritic dyke of this nappe is 27 Ma (sample no. 36). Late Cretaceous and Early Tertiary lithologies of the Laab nappe consistently give Early Miocene FT ages of 19 to 23 Ma. The samples from the Ybbsitz klippen zone belong to two different stratigraphic horizons. They give ages of 41 Ma in the Hubberg formation and 23 Ma in the Steinkeller formation.

Fission-track length distributions in the apatite samples

FT lengths have been measured in 28 apatite samples (Table 1). The detailed track-length distributions are presented in Trautwein (2000). Three different types of track-length distributions are distinguished: two unimodal distribution types with negative and positive skewness, respectively, and one bimodal type. The mean track length of the unimodal distribution with negative skewness ranges from 13.4 to 14.9 µm with a standard deviation between 1.2 and 2.1 µm. According to Gleadow et al. (1986), this kind of track-length distribution is typical of an intermediate to fast cooling history. In the case of a sedimentary basin series, this observation reflects cooling after total reset (Green 1986). The unimodal type with positive skewness is characterized by lengths of 11.1 to 12.5 µm with standard deviations in the narrow range of 1.7–1.9 µm. Following Green (1986), it can be suggested that such length distributions are caused by a prolonged stay in the partial annealing zone followed by fast cooling. The bimodal type varies between mean lengths of 11.9 and 13.3 µm with standard deviations of 2.0–2.7 µm. A bimodal distribution gives evidence for a more complex thermal history. The apatite ages of the samples

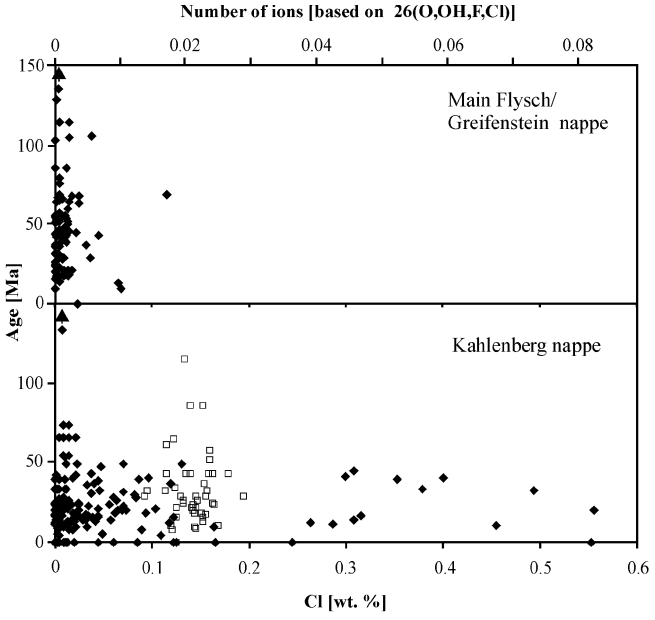

Fig. 5 Apatite FT ages versus chlorine content. No correlation of chlorine concentration and age is found. *Bold diamonds* sedimentary units, *open squares* picritic dyke

represent mixed ages and cannot be correlated with a geologic event of the rocks. The bimodality is caused by either a partial overprint or a prolonged stay in the partial annealing zone.

Fluorine and chlorine contents of apatites

The fluorine and chlorine contents were measured by electron microprobe in six apatite samples. The Cl content of the apatites is generally low (Fig. 5). Only few grains with substantial Cl content up to 0.56 wt% are present. The majority are almost pure fluorine apatites with minor contents of Cl and OH. The apatites of the picrite dyke have a mean Cl content of 0.14 wt%. They are of a 1:1 fluorine–hydroxyl composition.

The apatite grains show no correlation of composition with the single grain ages (Fig. 5). Therefore, the differences in age are only due to different thermal histories of the samples. This result is generally assumed for all samples.

Discussion and conclusions

Thermochronological significance of the apatite fission-track data

Due to incorporation of the RDFZ and YKZ into an Alpine-type fold-and-thrust belt, the two zones underwent burial and thermal overprint. The apatite FT ages show no correlation with the stratigraphic age of the samples. Kuckelkorn and Hiltmann (1992) found no correlation between the stratigraphic age and the maturity of organic matter in the western part of the RDFZ. Therefore, the thermal event affected the RDFZ during and after thrusting.

The apatites of the Kahlenberg and Laab nappe are consistently thermally overprinted. The ages range between 18.2 and 26.7 Ma. The age data set indicates that the samples were buried beneath the apatite partial annealing zone (APAZ 70 to 125 °C, after Gleadow et al. 1983) and are totally reset (Fig. 4; 'below APAZ'). Vitrinite reflectance data of Gmach (1999), measured in the same units, range between 0.6 and 0.97% Rr and are consistent with the thermal overprint determined by the apatite FT data.

The Main Flysch/Greifenstein nappe is characterized by widely scattering apatite ages (16.4 to 136.3 Ma, mean track lengths of 11.1 to 14.0 μm). The nappe shows rejuvenated apatite ages (16.4–33.9 Ma) in the west and along the southern margin of the RDFZ, where samples underwent total annealing before cooling (Fig. 4). Vitrinite reflectance values vary between 0.59 and 0.7% along the southern margin of the western RDFZ (Petschick 1989). In the central and eastern part of the RDFZ, mixed ages (41.3–92.9 Ma) reflecting moderate thermal overprint within the APAZ are common (Fig. 4). The apatite FT ages of these samples are younger than their sedimentation age.

Two further age groups are present, which contain age spectra with several age populations. One group is characterized by mean apatite FT ages older than the sedimentation age. The age spectra consist of two age populations with one age population younger and one older than the depositional age of the corresponding sample. The track-length distributions of these samples contain a high portion of shortened tracks. Therefore, heating into the APAZ can be assumed for these samples. In the Greifenstein nappe, this is in good agreement with vitrinite reflectance data (0.34–0.5% Rr; Gmach 1999).

The other group is represented by samples nos. 1 and 22, which show age spectra with no population younger than the sedimentation age. These samples were not buried into the partial annealing zone by a post-depositional event (Fig. 4). Thus, the grain ages provide information about the source rocks. The vitrinite reflectance value of the Wienerwald region (sample no. 22) is 0.36% Rr (Gmach 1999). The interpretation of the detrital ages is possible with the help of the detrital zircon FT ages from the same samples (Trautwein 2000).

The two samples of the Ybbsitz klippen zone indicate different levels of burial. There is no vertical trend, since the sample of the stratigraphically older Hubberg formation shows partial resetting, and the sample of the Steinkeller formation total resetting (Fig. 4).

Thermal modelling

Track-length distributions and FT ages were used to model the thermal history of 28 samples. Modelling was performed with the computer program AFTSolve of Ketcham et al. (2000), assuming all apatites to represent fluorine apatites.

The track-length data confirm the assumptions made on the basis of the apparent apatite ages, with two exceptions. Sample nos. 16 and 20 from the Reiselsberg formation pass the χ^2 test, although their length distributions are clearly bimodal, which points to a complex thermal history. Modelling displays either burial in the APAZ or below the APAZ (Fig. 4a).

In the Kahlenberg and Laab nappes, all samples show a similar thermal history. The pre-sedimentary history of the apatite grains was erased by burial to depths below the APAZ. The subsequent cooling rate was ~20 °C/Ma (Fig. 6a), which is reflected by moderate track-length shortening. Cooling started in Late Oligocene/Early Miocene times.

In contrast to the uniform thermal history of the Kahlenberg and Laab nappes in the Wienerwald area, the Main Flysch/Greifenstein nappe shows a heterogeneous cooling history. The thermal evolution is rather complex, and changes both along strike from west to east and from south to north are observed. The different time–temperature paths reflect the complexity of the flysch nappe pile and its evolution. Our data indicate that exhumation started in the central part of the RDFZ and propagated to the west and the east.

In the central part of the RDFZ, rocks of the Reiselsberg formation show local variations in age and degree of annealing. For two samples (12 and 14), modelling suggests burial into the APAZ (Fig. 6b), while there still was ongoing sedimentation in the flysch basin. Cooling already started in Late Cretaceous times (75–70 Ma), which is confirmed by model runs using the genetic algorithm of the Monte Trax program (Gallagher 1995).Three other samples of the Reiselsberg formation (nos. 13, 15 and 16) were buried much deeper and the apatite ages and track-length distributions reflect total reset. After maximum burial, the rocks cooled below 70 °C at a rate of ~10 °C/Ma starting in mid-Eocene time (Fig. 7).

Maastrichtian rocks of the Altlengbach formation in the central region are characterized by reaching a maximum burial in the partial annealing zone (sample nos. 6, 7 and 10). The fission-track ages and the length distributions reflect only partial reset (Fig. 6c). Cooling started between 50 and 30 Ma (Fig. 7).

In Cenomanian rocks (sample nos. 3 and 4) from the western part of the flysch zone, accelerated cooling from below the APAZ started around 40–30 Ma (cooling rate of ~6 °C/Ma) (Fig. 7). For the westernmost sample (no. 5), which was also buried beneath the partial annealing zone, cooling initiated by 17 Ma at the latest (cooling rate of ~6 °C/Ma) (Fig. 7).

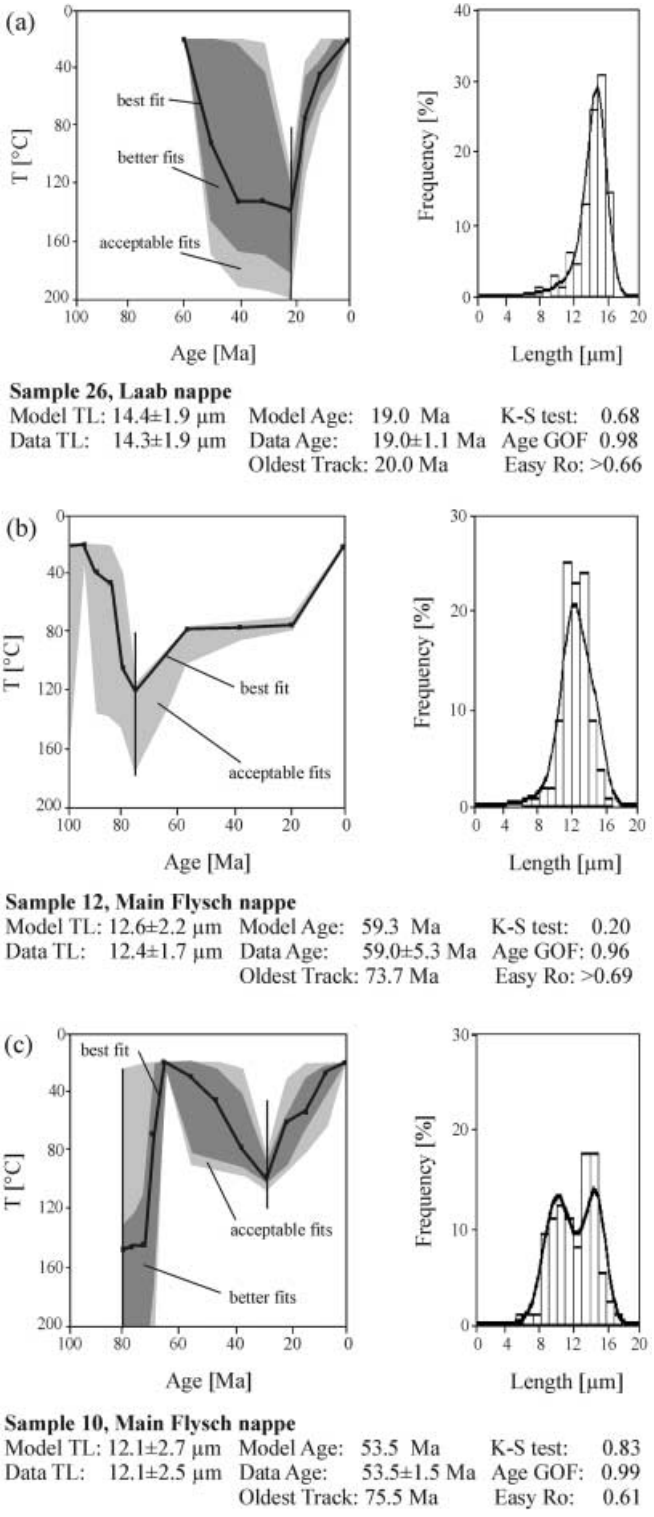

Fig. 6a–c Modelled temperature paths and track-length distributions. **a** Fast cooling after total resetting, representative of all samples from the Laab and Kahlenberg nappes. **b** Slow cooling, starting in Late Cretaceous. **c** Partial resetting. *K–S* Kolmogoroff–Smirnow

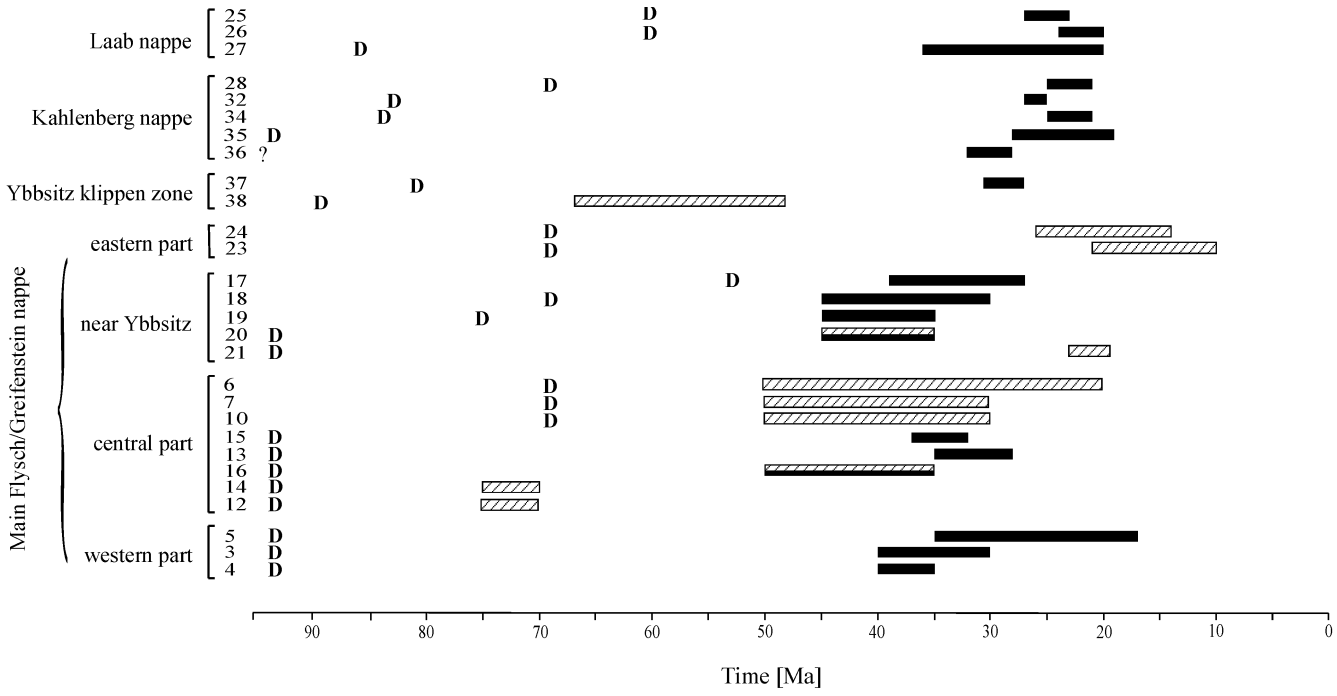

Fig. 7 Overview of modelling results for apatite FT data from the Rhenodanubian flysch. *Bars* show the time range for onset of cooling. *D* approx. deposition age, *striped bars* in APAZ, *black bars* below APAZ

In the eastern part of the Main Flysch nappe, thermal modelling reveals a cooling history that started around 45–36 Ma (Fig. 7), with varying cooling rates. The rocks of the Reiselsberg formation and of the Altlengbach formation (sample nos. 19 and 20) were buried below the APAZ and experienced total reset. The Late Maastrichtian sample of the Altlengbach formation (sample no. 18) did not suffer complete reset, but only reached the partial annealing zone. A similar cooling history as determined in the Kahlenberg and Laab nappes is found for sample no. 17 of the Main Flysch nappe.

The Greifenstein nappe (sample nos. 23 and 24) and sample no. 21 of the Main Flysch nappe underwent a thermal history different from the Kahlenberg and Laab nappes. The sediments experienced continuous burial and heating to 100 °C. Modelling suggests a prolonged stay in the partial annealing zone followed by cooling with a rate of ~4 °C/Ma starting around 20–14 Ma.

The sample of the Hubberg formation of the YKZ (no. 38) displays burial into the partial annealing zone. Cooling at a rate of ~2 °C/Ma starts around 60–50 Ma. The sample of the Steinkeller formation (no. 37) shows a similar cooling pattern to that observed in samples of the Kahlenberg and Laab nappes with the same stratigraphic age. Cooling started after total resetting around 30–27 Ma at a rate of ~10 °C/Ma.

Evolution of the Rhenodanubian accretionary wedge – nappe stacking and exhumation

Modelling of the FT data reveals a very detailed pattern of burial and cooling histories within the studied rock units (Fig. 8). The burial depths of the sediments vary along and also perpendicular to the strike of the RDFZ and are not even uniform at the local scale (Fig. 4a, c). The different cooling patterns of the samples can be explained by successive and differential accretion and exhumation.

Following Hasebe et al. (1993), we assume a geothermal gradient of 20 °C/km for the Rhenodanubian flysch wedge. In this case, the apatite data give evidence for a minimum burial depth of ~6 km for those samples which experienced total resetting of apatite FT ages after sediment deposition (lower boundary of APAZ at 125 °C). Since the zircon FT ages are not reset (Trautwein 2000), the exposed flysch units did not reach the zircon partial annealing zone (220–320 °C, Tagami et al. 1998), i.e. they were not buried deeper than ~11 km. A cover of the Rhenodanubian flysch wedge by the structurally higher Northern Calcareous Alps would result in an overburden of 5–6 km. Adding of additional (now eroded) material (NCA and Augenstein sediments; Frisch et al. 2001) would lead to burial temperatures sufficient for complete apatite FT annealing.

Our data show that nappe stacking processes were active from Maastrichtian to Miocene times. Figure 7 compiles the modelled onset of cooling for the different flysch slices. Our data suggest the following tectonic evolution for the Rhenodanubian flysch zone.

In the central part of the Rhenodanubian flysch zone, accretionary processes had already started in

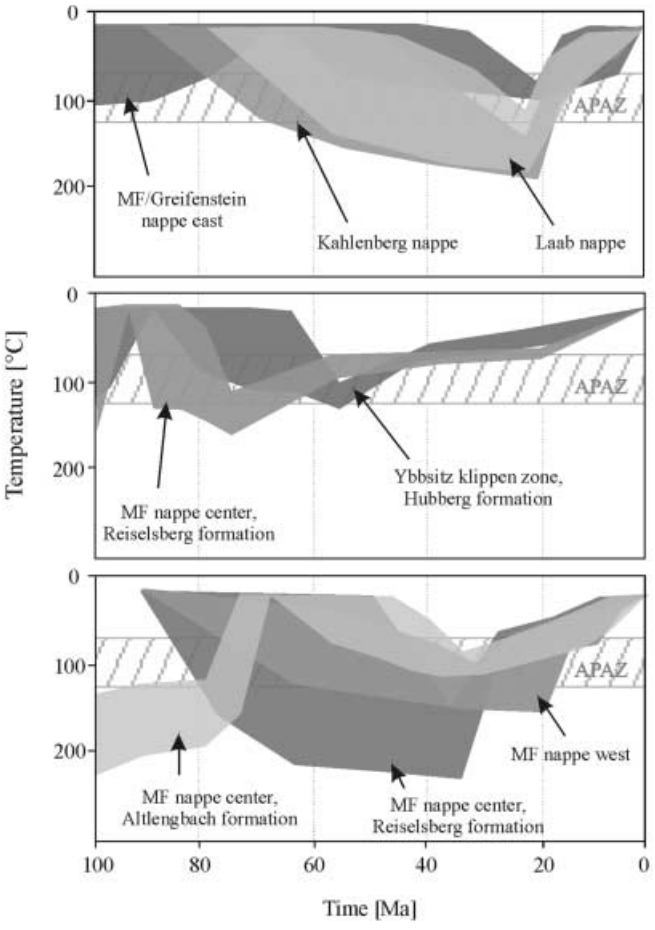

Fig. 8 Summarized T–t paths for the nappes of the Rhenodanubian flysch and the Ybbsitz klippen zone; *APAZ* apatite partial annealing zone; *MF* Main Flysch

pre-Maastrichtian time, as cooling of the Reiselsberg formation began at 75–70 Ma (Figs. 6b, 7, 8). The data disprove previous assumptions that the Rhenodanubian flysch was deposited in a dormant trench without subduction activity during deposition (Hesse 1982), which lasted until Early Eocene in the central area of the RDFZ (Egger 1989). On the contrary, accretion in a subduction zone is indicated, as suggested by Frisch (1978, 1979). An active basin setting was also presumed by Hesse (1972). The Cenomanian sediments were dragged down a subduction zone and were underplated due to ongoing accretion (e.g. Moore 1989; Platt 1986), which initiated steady cooling and exhumation of this flysch slice during Maastrichtian times. Early accretion is also indicated for the Hubberg formation sample from the Ybbsitz klippen zone (Fig. 7).

Modelling of apatite FT data suggests that accretion propagated from the Salzburg–Ybbsitz area to the west and to the east. The time of incorporation of the sediments into the wedge and thus their time–temperature history along strike were different, as the continental margin of the bending European plate was neither straight (Malzer et al. 1993; Wagner 1998) nor characterized by a homogeneous strength. This may be due to the Bohemian spur, which actually protruded beneath the Eastern Alps in the area around Ybbsitz (Fig. 1). The Bohemian spur may have reached the Alpine front already in Late Cretaceous time.

In the Salzburg–Ybbsitz area, cooling of Cenomanian to Early Paleocene rocks started in Middle Eocene times (Fig. 7). West of Salzburg, cooling of the Reiselsberg sediments started in Middle Eocene to Early Oligocene time (Fig. 7). The Altlengbach sediments in the central area and Campanian to Eocene sediments of the RDFZ and the YKZ in the Ybbsitz area show an onset of cooling in Late Eocene/Early Oligocene time (Fig. 7), due to the ongoing process of accretion. We suppose that these ages reflect the time of underplating (e.g. Platt 1986; Moore 1989) of the RDFZ by the European continental margin, incorporating Ultrahelvetic slices into the nappe stack.

In the Wienerwald region the exhumation of the Kahlenberg and Laab nappes was initiated during the Late Oligocene to Early Miocene, and in the Greifenstein nappe during the Early to Middle Miocene. This is linked to foreland imbrications in the eastern RDFZ that stopped in the Early Miocene (Wagner 1998). The evolution of the nappe stack in the Wienerwald area can be explained as follows.

From a detailed provenance study based on zircon morphology and fission-track data, Trautwein (2000) deduced a paleogeographic arrangement of the depositional areas of the RDFZ in the Wienerwald area, which was already considered by Oberhauser (1995). According to this reconstruction, the Laab basin (the later Laab nappe) occupied the northernmost position (Fig. 9a), since the zircon data reflect a source area situated in stable Europe (e.g. Bohemian massif). The Main Flysch basin was situated to the south of the Laab basin. Sedimentation terminated in Paleocene times in the southernmost area of the Main Flysch basin (the later Kahlenberg nappe), and it was sealed by overthrusting and incorporation into the accretionary wedge. In the northern Main Flysch basin (the later Greifenstein nappe) and in the Laab basin sedimentation lasted until Eocene, before the nappe was incorporated into the wedge. The sedimentary sequence was buried, and the apatites of the Laab and Kahlenberg nappes experienced total annealing. To place the Laab basin on top of the northern Main Flysch basin, resulting in the present nappe configuration with the Greifenstein nappe in the north overthrusted by the Laab and Kahlenberg nappes, an out-of-sequence thrust is proposed (Fig. 9a). Figure 9b depicts the evolution of the nappe pile on the basis of other paleogeographical models, with the Laab basin in a middle position (e.g. Faupl and Wagreich 1992). The model presented in Fig. 9a is in accordance with the zircon fission-track data (Trautwein 2000) and the

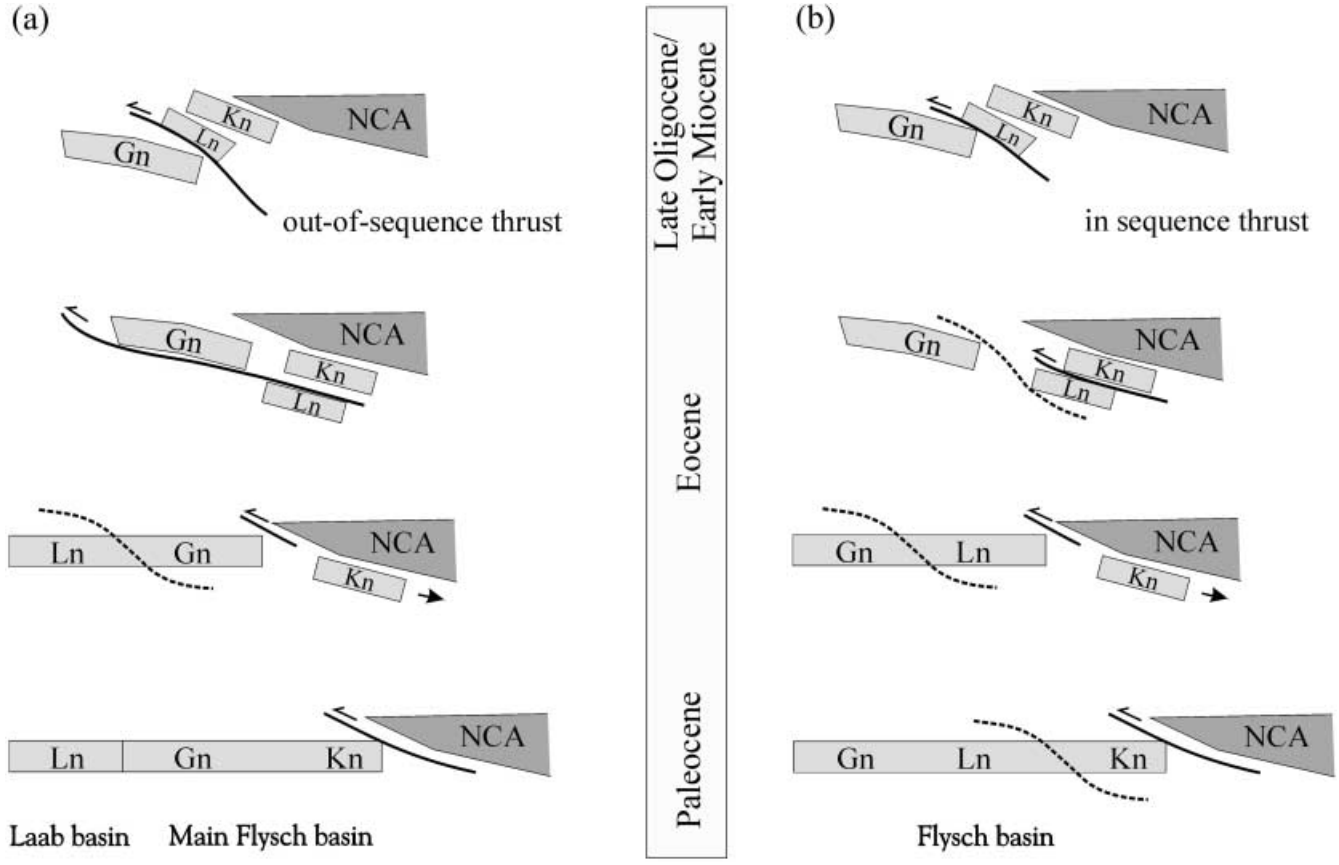

Fig. 9 Tectonic evolution of the Wienerwald nappe pile. **a** Assuming a northern position of the Laab basin (Trautwein 2000). An out-of-sequence thrust is necessary to achieve the present-day nappe configuration and to be in accordance with our apatite FT data. **b** Based on paleogeographical considerations of others (e.g. Faupl and Wagreich 1992) and in accordance with our apatite FT data. *Ln* Laab nappe, *Kn* Kahlenberg nappe, *Gn* Greifenstein nappe, *NCA* Northern Calcareous Alps

apatite FT data of the present study and is therefore preferred.

An additional influence on the exhumation of the Wienerwald nappes is the large-scale E–W extrusion that began during Early to Middle Miocene time ('lateral tectonic extrusion', Ratschbacher et al. 1991; Frisch et al. 1998). The ductile deformable sediments of the RDFZ and the Molasse zone accommodated part of the shear (Meschede and Decker 1993) between the NCA, which experienced ~50% stretching, and the unstretched foreland basement. Lateral extrusion was accompanied by an exhumation pulse, as reflected in the Late Oligocene/Early Miocene cooling paths of the flysch samples (Fig. 8).

Acknowledgements For fruitful discussions, we are very grateful to Joachim Kuhlemann, Franz Moser, Reinhard Sachsenhofer, Martina Schwab and Cornelia Spiegel. Many thanks to Claudia Hanfland for the arduous job of sample preparation. We are much obliged to Meinert Rahn and Wilfried Winkler for their constructive reviews. The final review by Neil Mancktelow improved the manuscript; our thanks to him. Financial support from the German Science Foundation, the German Academic Exchange Service and the state Baden-Württemberg is gratefully acknowledged.

References

Bhandari N, Bhat SG, Lal D, Rajagopalan G, Tamhane ASJ, Venkatavaradan VS (1971) Fission fragment tracks in apatite: recordable track lengths. Earth Planet Sci Lett 13:191–199

Decker K (1990) Plate tectonic and pelagic facies: Late Jurassic to Early Cretaceous deep-sea sediments of the Ybbsitz ophiolite unit (Eastern Alps, Austria). Sediment Geol 67:85–99

Egger H (1989) Zur Geologie der Flyschzone im Bundesland Salzburg. Jahrb Geol B-A 132:375–395

Egger H (1990) Zur paläogeographischen Stellung des Rhenodanubischen Flysches (Neokom–Eozän) der Ostalpen. Jahrb Geol B-A 133:147–155

Egger H (1992) Zur Geodynamik und Paläogeographie des Rhenodanubischen Flysches (Neokom – Eozän) der Ostalpen. Z Dtsch Geol Ges 143:51–65

Egger H (1995) Zur Lithostratigraphie der Altlengbach-Formation und der Anthering-Formation im Rhenodanubischen Flysch (Ostalpen, Penninikum). Neues Jahrb Geol Paläont 196:69–91

Exner CE, Kirchner EC (1982) Zum Chemismus einiger basischer Gesteine aus dem Flysch und Klippenraum. Jahresber 1981 Hochschulschwp S 15/3:55–59

Faupl P (1996) Tiefwassersedimente und tektonischer Bau der Flyschzone des Wienerwaldes. Exkursionsführer Sediment 96, Wien

Faupl P, Wagreich M (1992) Cretaceous flysch and pelagic sequences of the Eastern Alps: correlation, heavy minerals, and palaeogeographic implications. Cretaceous Res 13:387–403

Frisch W (1978) A plate tectonic model of the Eastern Alps. In: Cloos H, Roeder DH, Schmidt K (eds) Alps, Apennines, Hellenides. Geodynamic investigations along geotraverses. Schweizerbart, Stuttgart, pp 167–172
Frisch W (1979) Tectonic progradation and plate tectonic evolution of the Alps. Tectonophysics 60:121–139
Frisch W, Kuhlemann J, Dunkl I, Brügel A (1998) Palinspastic reconstruction and topographic evolution of the Eastern Alps. Mem Sci Geol Padova 51:3–23
Frisch W, Kuhlemann J, Dunkl I, Székely B (2001) The Dachstein paleosurface and the Augenstein Formation in the Northern Calcareous Alps – a mosaic stone in the geomorphological evolution of the Eastern Alps. Int J Earth Sci DOI 10.007/s005310000189 (this issue)
Galbraith R (1981) On statistical models for fission track counts. Math Geol 13:471–488
Gallagher K (1995) Evolving temperature histories from apatite fission-track data. Earth Planet Sci Lett 136:421–435
Gleadow AJW (1981) Fission track dating methods: what are the real alternatives? Nucl Tracks 5:3–14
Gleadow AJW, Duddy IR, Lovering JF (1983) Fission track analysis: a new tool for the evaluation of thermal histories and hydrocarbon potential. Aust Petrol Explor Assoc J 23:93–102
Gleadow AJW, Duddy IR, Green PF, Lovering JF (1986) Confined fission track length in apatite: a diagnostic tool for thermal history analysis. Contrib Mineral Petrol 94:405–415
Gmach H (1999) Thermische Reife der Flyschzone im Bereich des Wienerwaldes und der Flyschanteile nördlich der Donau und deren Einfluß auf die Kohlenwasserstoffgenese am Rand des Wiener Beckens. Diploma Thesis, Leoben
Green PF (1981) A new look at statistics in the fission track dating. Nucl Tracks 5:77–86
Green PF (1986) On the thermo-tectonic evolution of Northern England: evidence from fission track analysis. Geol Mag 123:493–506
Green PF (1988) The relationship between track shortening and fission track age reduction in apatite: combined influences of inherent instability, annealing anisotropy, length bias and system calibration. Earth Planet Sci Lett 89:335–352
Green PF, Duddy IR, Gleadow AJW, Tingate PR, Laslett GM (1986) Thermal annealing of fission tracks in apatite 1. A qualitative description. Chem Geol (Iso Geosci Sect) 59:237–253
Green PF, Duddy IR, Gleadow AJW, Lovering JF (1989) Apatite fission-track analysis as a paleotemperature indicator for hydrocarbon exploration. In: Naeser ND, McCulloh TH (eds) Thermal history of sedimentary basins – methods and case histories. Springer, Berlin Heidelberg New York, pp 181–196
Hasebe N, Tagami T, Nishimura S (1993) Evolution of the Shimanto accretionary complex: a fission-track thermochronologic study. Geol Soc Am Spec Pap 273:121–136
Hejl E, Grundmann G (1989) Apatit-Spaltspurdaten zur thermischen Geschichte der Nördlichen Kalkalpen, der Flysch- und Molassezone. Jahrb Geol B-A 132:191–212
Hesse R (1972) Lithostratigraphie, Petrographie und Entstehungsbedingungen des bayerischen Flysches: Unterkreide. Geol Bavarica 66:148–222
Hesse R (1973) Flysch-Gault und Falknis-Tasna-Gault (Unterkreide): Kontinuierlicher Übergang von der distalen zur proximalen Flyschfazies auf einer penninischen Trogebene der Alpen. Geol Paleont Marburg, Sb 2
Hesse R (1982) Cretaceous–Palaeogene Flysch Zone of the East Alps and Carpathians: identification and plate-tectonic significance of 'dormant' and 'active' deep-sea trenches in the Alpine–Carpathian Arc. In: Leggett JK (ed) Trench–forearc geology. Geol Soc Lond Spec Publ 10:471–494
Hurford AJ, Fitch FJ, Clarke A (1984) Resolution of the age structure of the detrital zircon populations of two Lower Cretaceous sandstones from the Weald of England by fission track dating. Geol Mag 121:269–396
Ketcham RA, Donelick RA, Donelick MB (2000) AFTSolve: a program for multi-kinetic modeling of apatite fission-track data. Geol Mat Res 2(1):1–32
Kuckelkorn KF, Hiltmann W (1992) New maturity interpretation of alpine overthrusting, Bavaria, Germany. In: Spencer AM (ed) Generation, accumulation and production of Europe's hydrocarbons II. Eur Assoc Petrol Geosci Spec Publ 2:177–184
Malzer O, Rögl F, Seifert P, Wagner L, Wessely G, Brix F (1993) Die Molassezone und deren Untergrund. In: Brix F, Schultz O (eds) Erdöl und Erdgas in Österreich. Naturhist Museum Wien, pp 281–358
Mattern F (1998) Lithostratigraphie und Fazies des Reiselsberger Sandsteins: sandreiche, submarine Fächer (Cenomanium–Turonium, westlicher Rhenodanubischer Flysch, Ostalpen). Berliner Geowiss Abh A198:1–133
Meschede M, Decker K (1993) Störungsflächenanalyse am Nordrand der Ostalpen – ein Vergleich numerischer und graphischer Methoden. Z Dtsch Geol Ges 144:419–433
Moore JC (1989) Tectonics and hydrogeology of accretionary prisms: role of décollement zone. J Struct Geol 11:95–106
Oberhauser R (1995) Zur Kenntnis der Tektonik und der Paläogeographie des Ostalpenraumes zur Kreide-, Paleozän- und Eozänzeit. Jahrb Geol B-A 138:369–432
Petschick R (1989) Zur Wärmegeschichte im Kalkalpin Bayerns und Nordtirols (Inkohlung und Illit-Kristallinität). Frankf Geowiss Arb C10:1–259
Platt JP (1986) Dynamics of orogenic wedges and the uplift of high-pressure metamorphic rocks. Bull Geol Soc Am 97:1037–1053
Plöchinger B, Prey S (1993) Der Wienerwald. Samml Geol Führer 59. Borntraeger, Berlin
Prey S (1980) Helvetikum, Flysche und Klippenzone von Salzburg bis Wien. In: Oberhauser R (ed) Der geologische Aufbau Österreichs. Springer, Wien, pp 189–217
Prey S (1983) Die Deckschollen der Kahlenberger Decke von Hochrotherd und Wolfsgraben im Wienerwald. Verh Geol B-A, Wien, 1982:243–250
Rad U von (1972) Zur Sedimentologie und Fazies des Allgäuer Flysches. Geol Bavarica 66:92–147
Ratschbacher L, Frisch W, Linzer H-G (1991) Lateral extrusion in the Eastern Alps, Part 2: structural analysis. Tectonics 10:257–271
Ruttner A, Schnabel W (1988) Geologische Karte der Republik Österreich 1:50.000, Blatt 71 Ybbsitz. Geol B-A, Wien
Schnabel W (1979) Geologie der Flyschzone einschließlich der Klippenzone. Arb Geol B-A 1979:17–42
Schnabel W (1992) New data on the Flysch Zone of the Eastern Alps in the Austrian sector and new aspects concerning the transition to the Flysch Zone of the Carpathians. Cretaceous Res 13:405–419
Tagami T, Galbraith RF, Yamada R, Laslett GM (1998) Revised annealing kinetics of fission tracks in zircon and geological implications. In: Van den haute P, Corte F de (eds) Advances in fission-track geochronology. Kluwer , Dordrecht, pp 99–112
Trautwein B (2000) Detritus provenance and thermal history of the Rhenodanubian flysch zone: mosaic stones for the reconstruction of the geodynamic evolution of the Eastern Alps. Tübinger Geowiss Arb A59:1–68
Wagner L (1998) Tectono-stratigraphy and hydrocarbons in the Molasse Foredeep of Salzburg, Upper and Lower Austria. In: Mascle A, Puigdefàbregas C, Luterbacher HP, Fernàndez M (eds) Cenozoic foreland basins of Western Europe. Geol Soc Lond Spec Publ 134:339–369
Wagner GA, Van den haute P (1992) Fission-track dating. Enke, Stuttgart
Winkler W, Wildi W, van Stuijvenberg J, Caron C (1985) Wägital-Flysch et autres flysches penniques en Suisse Centrale; Stratigraphie, sédimentologie et comparaisons. Eclog Geol Helv 78:1–22